Charged and Neutral NO_3 Isomers from the Ionization of NO_x and O_3 Mixtures

Fulvio Cacace,*[a] Giulia de Petris,*[a] Marzio Rosi,[b] and Anna Troiani[a]

Abstract: Mass spectrometric techniques have been utilized in conjunction with theoretical methods to detect and characterize new species formed upon ionization of gaseous mixtures containing ozone and an NO_x oxide. NO_5^+ as well as isomeric NO_4^+ and NO_3^+ ions have been identified. Moreover, utilization of neutralization reionization mass spectrometry (NRMS) has provided strong evidence for, if not a conclusive demonstration of, the existence of a new NO_3 isomer, in addition to the long-known trigonal radical, as a gaseous species with a lifetime in excess of ≈ 1 μs.

Keywords: gas-phase reactions · mass spectrometry · nitrogen oxides · ozone

Introduction

Much of our recent activity has focused on the study of the ionic chemistry of mixtures containing traces of O_3 and simple inorganic compounds diluted in atmospheric gases.[1] The reasons for these studies are manifold. One stems from the currently increasing recognition of the role of ionization phenomena promoted in all regions of the atmosphere by different agents, both natural (solar radiation, cosmic rays, radioactive emanation, lightning, thunderstorm coronas) and anthropogenic (coronas caused by high-voltage power lines, wake flow-field behind re-entry vehicles, etc.).[2, 3] Furthermore, the ionic reactions occurring in atmospheric-pressure gases are of direct interest to the development of plasma technology for the removal of trace contaminants from industrial effluents, especially with regard to the effects of additives.[4] All the ionization phenomena produce high local concentrations of ozone, and this consideration, together with the great current interest in all processes responsible for the formation and the destruction of O_3, justifies its choice as a component of all gaseous mixtures previously investigated.

[a] Prof. Dr. G. de Petris, Prof. Dr. F. Cacace, Dr. A. Troiani
Dipartimento di Studi di Chimica e Tecnologia
delle Sostanze Biologicamente Attive
Università "La Sapienza", P.le Aldo Moro 5
00185 Roma (Italy)
Fax: (+39) 6-49913602
E-mail: giulia.depetris@uniroma1.it

[b] Prof. Dr. M. Rosi
Dipartimento di Ingegneria Civile ed Ambientale
Sezione Tecnologie Chimiche e Materiali per l'Ingegneria
Università di Perugia, Via Duranti
06131 Perugia (Italy)
Fax: (+39) 75-5855606
E-mail: marzio@thch.unipg.it

As an extension of the above studies, we report here the results of a joint mass spectrometric and theoretical investigation of the ionic chemistry promoted by the ionization of mixtures containing O_3 and NO_x oxides. These molecules are involved in globally relevant tropospheric and stratospheric processes, and their life and fate are strictly related,[2] owing to the manifold interactions involving both neutral and charged species.[2, 3] As an example, the tropospheric ozone balance, crucial to the problem of the oxidizing capacity of the troposphere, strictly depends on the available NO_x concentration, the major source of tropospheric ozone being the photolysis of nitrogen dioxide. Moreover, it is long known that NO_x oxides activate catalytic cycles that are effective in the depletion of stratospheric ozone. Passing to plasma technology, the strict link between O_3 and NO_x oxides is even more evident, for example, recent kinetic studies have demonstrated the formation and the role of ozone in barrier discharges utilized for exhaust gas purification.[5] A specific goal of the present study, as of previous related investigations, is the detection and the characterization of the intermediates and the products of the ionic processes of interest, in particular of previously unknown species, including the NO_4^+ and NO_5^+ ions and new NO_3^+ isomers. Indeed, despite its importance, to the best of our knowledge, no experimental studies of the NO_3^+ ion have been reported, and the theoretical analysis of its equilibrium structure and of the relative stability of its isomers is seriously affected by symmetry-breaking effects.[6] The same applies to the $NO_3^{\cdot}$ radical, the major tropospheric night-time oxidant, whose theoretical study is still the focus of active interest.[7] From the experimental standpoint, studies based on IR spectroscopy have provided circumstantial evidence for the existence of a $NO_3^{\cdot}$ isomer with OONO connectivity, in addition to the well-established trigonal radical.[8] The assignment has been questioned, and several

  0947-6539/02/0824-5684 $ 20.00+.50/0

theoretical studies predict that the OONO radical should be unstable or only marginally stable.[7a,c] In the present study we have addressed the problem utilizing neutralization reionization mass spectrometry (NRMS), a powerful technique for the detection of elusive molecules and radicals.[9]

Results

Formation and structural analysis of the NO_5^+ ion: The NO_5^+ ion (m/z 94) is observed in the chemical ionization (CI) spectra of $NO_2/O_3/O_2$ mixtures. It is most probably formed by reaction (1), which occurs at sufficiently high pressures to ensure collisional stabilization of the adduct.

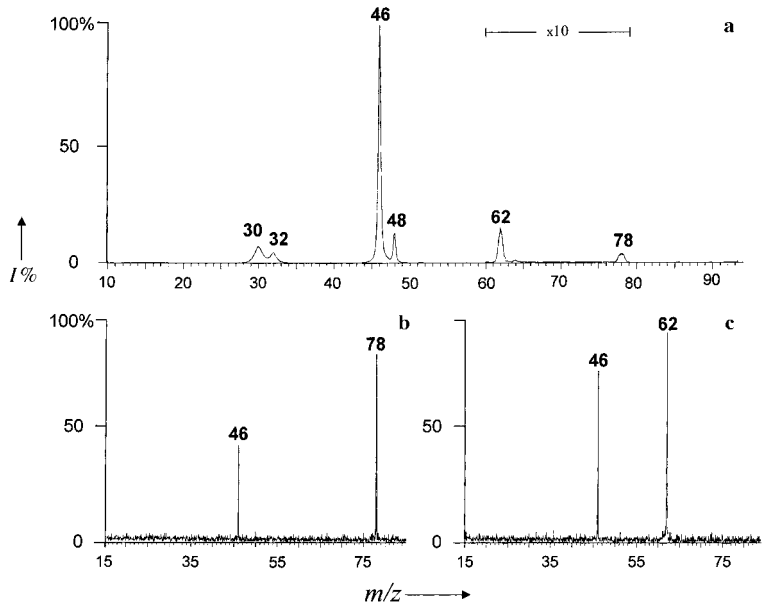

Figure 1. a) CAD spectrum of the NO_5^+ ion (m/z 94), b) CAD-TOF mass spectrum of the m/z 78 daughter ion from m/z 94, c) CAD-TOF mass spectrum of the m/z 62 daughter ion from m/z 94.

$$NO_2^+ + O_3 \xrightarrow{M} NO_5^+ \quad (1)$$

The CAD (collisionally activated dissociation) spectrum of the mass-selected NO_5^+ ion, reported in Figure 1a, shows the m/z 46 (NO_2^+) peak as the most abundant fragment, with minor abundances of m/z 30 (NO^+), m/z 32 (O_2^+) and m/z 48 (O_3^+) fragments. Additional peaks of m/z 78 (NO_4^+) and m/z 62 (NO_3^+) are structurally informative, despite their low intensity. Indeed, when mass- and energy-reselected and analyzed in the TOF section of the mass spectrometer, their MS^3 (multistage spectrometry) spectra (Figure 1b and 1c) display the m/z 46 fragment. This suggests that the NO_5^+ ion and its fragments all have a O_n-NO_2 ($n = 1-3$) connectivity.

$$[NO_5^+]\ (O_3\text{-}NO_2) \xrightarrow{CAD} \begin{cases} \xrightarrow{-O} [NO_4^+]\ (O_2\text{-}NO_2) \xrightarrow{MS/MS} NO_2^+ + O_2 & (1a) \\ \xrightarrow{-O_2} [NO_3^+]\ (O\text{-}NO_2) \xrightarrow{MS/MS} NO_2^+ + O & (1b) \end{cases}$$

Formation and structural analysis of the NO_4^+ ion: These ions are obtained by CI of $NO/O_3/O_2$ and $NO_2/O_3/O_2$ mixtures. Reaction (2) is the major process in the CI of $NO/O_3/O_2$ mixtures.

$$NO^+ + O_3 \rightarrow NO_4^+ \quad (2)$$

To prevent conceivable reactions between the neutral species, ozone and nitric oxide were introduced into the source through separate inlets, and indeed only a small intensity ($<5\%$) of the NO_2^+ ion was observed under these conditions. Therefore, the possible occurrence of reaction (3)

$$NO_2^+ + O_3 \rightarrow NO_4^+ + O \quad (3)$$

can only account for a minor fraction, if any, of the NO_4^+ ionic population. The other conceivable route [reaction (4)] can be

$$NO_2^+ + O_2 \rightarrow NO_4^+ \quad (4)$$

excluded, based on the results of separate experiments, involving the CI of NO_2/O_2 mixtures, showing that NO_2^+ is unreactive towards O_2.

The CAD spectrum of the NO_4^+ population from reaction (2), shown in Figure 2a, displays the m/z 30 (NO^+) peak as the most abundant fragment, which denotes a O_3-NO connectivity, different than that of the NO_4^+ fragment obtained from the dissociation of NO_5^+ [reaction (1a)].

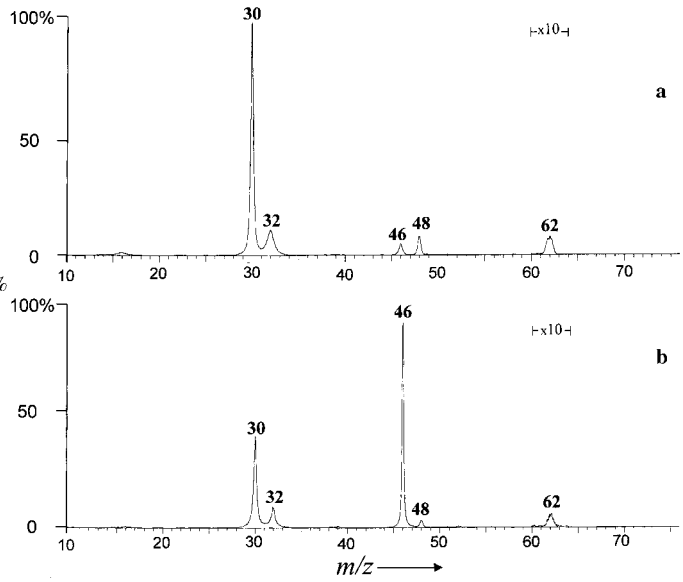

Figure 2. CAD spectrum of the NO_4^+ ion (m/z 78), a) from the CI of $NO/O_3/O_2$, b) from the low-pressure CI of $NO_2/O_3/O_2$.

In the case of the CI of $NO_2/O_3/O_2$ mixtures, the simultaneous occurrence of reactions (2) and (3) is more significant

  0947-6539/02/0824-5685 $ 20.00+.50/0

as a result of the relatively high abundance of NO^+ in this plasma. Indeed, in this case, the CAD spectrum of the NO_4^+ population changes depending on the NO_2^+/NO^+ ratio, which is in turn affected by the pressure in the source. At the highest attainable pressure (0.1–0.3 Torr), the NO_2^+/NO^+ ratio approaches unity and the spectrum is the same as that reported in Figure 2a. This suggests that, under these conditions, NO^+ effectively competes with NO_2^+, and reaction (2) still predominates. At lower pressures ($NO_2^+/NO^+ \approx 10$) the spectrum changes, displaying the peak of m/z 46 as the most abundant fragment (Figure 2b). By independent experiments, we have excluded the possibility that metastable components affect the abundance ratio of the CAD peaks, and hence the different CAD spectra can be ascribed to the presence of different NO_4^+ ions, one of O_3-NO and the other one of O_2-NO_2 connectivity, the latter being the same species formed from the fragmentation of NO_5^+ [reaction (1a)]. The occurrence of NO_4^+ isomers is conclusively confirmed by the MS^3 spectra of their m/z 62 daughter ions, displaying peaks of m/z 30 and 46, respectively, which in turn gives a first hint of the existence of different NO_3^+ isomers [reactions (2a) and (3a)].

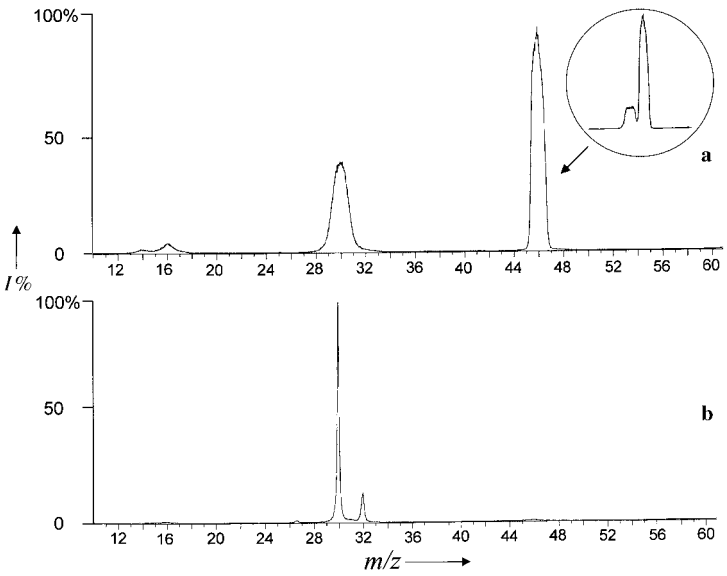

Figure 3. CAD spectrum of the NO_3^+ ion (m/z 62), a) from the EI of NO_3 (see text), b) from the CI of NO/O_2.

$$[O_3\text{-}NO]^+ \xrightarrow[CAD]{-O} [NO_3]^+ \xrightarrow{MS/MS} NO^+ + O_2 \quad (2a)$$

$$[O_2\text{-}NO_2]^+ \xrightarrow[CAD]{-O} [NO_3]^+ \xrightarrow{MS/MS} NO_2^+ + O_2 \quad (3a)$$

Formation and structural analysis of the NO_3^+ ion: The first indirect evidence for different NO_3^+ isomers comes from the dissociation of NO_5^+ and NO_4^+, and suggests the existence of at least two species, one of O-NO_2 connectivity from NO_5^+ and $[O_2\text{-}NO_2]^+$ [reactions (1b) and (3a)], the other one of O_2-NO connectivity from $[O_3\text{-}NO]^+$ [reaction (2a)].

NO_3^+ species have been generated *directly* in the ion source by the processes given in reactions (5)–(7):

$$NO_3^{\cdot} \xrightarrow{EI} NO_3^+ + e^- \quad (5)$$

$$NO^+ + O_2 \xrightarrow{CI} NO_3^+ \quad (6)$$

$$NO_2^+ + O_3 \xrightarrow{CI} NO_3^+ + O_2 \quad (7)$$

Based on the known structure of the parent radical, the NO_3^+ ion from reaction (5) can be taken as a model ion of trigonal structure. $NO_3^{\cdot}$ was produced in situ by reaction of NO_2 with O_3, according to an established procedure,[10] and ionized by low-energy (40 eV) electron ionization (EI). The CAD spectrum, shown in Figure 3a, displays wide Gaussian-type peaks of m/z 46 (NO_2^+) and m/z 30 (NO^+), consistent with the expected O-NO_2 connectivity. In addition, the MIKE (mass-analyzed ion kinetic energy) spectrum shows a dish-topped peak of m/z 46, characterized by a large kinetic energy release (KER). It is also detectable in the CAD spectrum of Figure 3a (see the inset) when the collision cell is floated to a 1 keV potential, which allows one to discriminate between unimolecular dissociation of metastable ions and collisional dissociation of stable ions.

The CAD spectrum of the NO_3^+ ion formed from reaction (6) by high-pressure CI of NO/O_2 mixtures is shown in Figure 3b. It displays narrow peaks of m/z 30 (NO^+) and m/z 32 (O_2^+); this denotes a O_2-NO connectivity. In addition, if $^{15}NO/O_2$, $NO/^{18}O_2$, or $^{15}NO/^{18}O_2$ mixtures are employed, the CAD spectra of the resulting $^{15}NO_3^+$, $NO^{18}O_2^+$, and $^{15}NO^{18}O_2^+$ ions, respectively, have peaks displaced to m/z 31 and 32 ($^{15}NO^+$, O_2^+), m/z 30 and 36 (NO^+, $^{18}O_2^+$), and m/z 31 and 36 ($^{15}NO^+$, $^{18}O_2^+$), respectively. The lack of isotopic mixing points to a structure in which the NO and O_2 moieties retain their discrete identity.

With regard to reaction (7), the CAD spectrum of the NO_3^+ ions formed by high-pressure CI of $NO_2/O_3/O_2$ mixtures considerably changes as to the nature, abundance, and shape of the peaks, depending on the pressure and the NO_2^+/NO^+ ratio in the source. Actually, as noted for the NO_4^+ ion, the occurrence of the alternative formation process (6) cannot be excluded, owing to the significant abundance of NO^+ in the NO_2/O_3 CI. Figure 4 illustrates two typical CAD spectra recorded under different pressure conditions. At the highest attainable pressure (Figure 4a), the spectrum displays narrow peaks of m/z 46 and m/z 30, with a minor fragment of m/z 32. Under these conditions, the abundance ratio of the two major peaks of m/z 46 and 30 critically depends on the NO_2^+/NO^+ ratio in the CI source: a slight increase of the NO^+ ion in the source causes a significant increase of the NO^+ fragment in the CAD spectrum. Having excluded the presence of metastable components, the differences observed can only be traced to different NO_3^+ ions, whose composition in the mixed population assayed changes as a function of the relative amounts of the NO^+ and NO_2^+ charged reactants of reac-

0947-6539/02/0824-5686 $ 20.00+.50/0 *Chem. Eur. J.* **2002**, *8*, No. 24

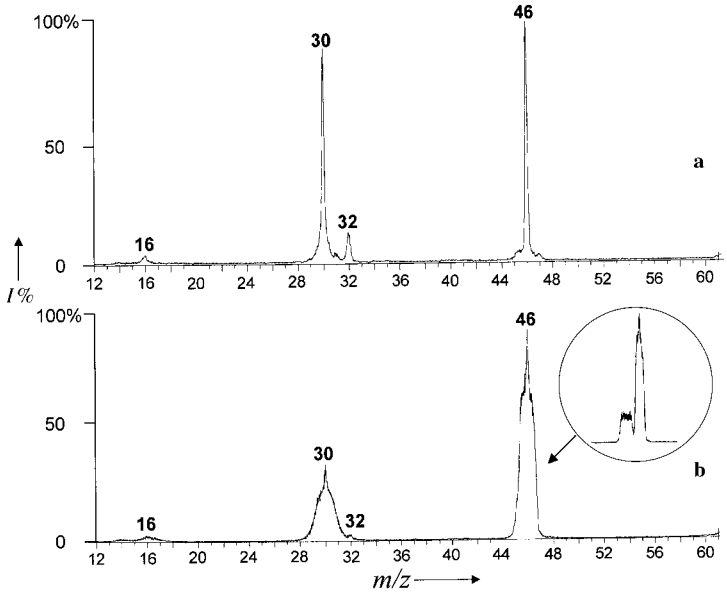

Figure 4. CAD spectrum of the NO_3^+ ion (m/z 62), a) from the high-pressure CI of $NO_2/O_3/O_2$, b) from the low-pressure CI of $NO_2/O_3/O_2$ (see text).

tions (6) and (7), respectively. Supporting evidence is provided by the minor peak of m/z 32, whose intensity strictly follows that of the peak of m/z 30, reaching its maximum at the I_{30}/I_{32} ratio observed in the CAD spectrum of the ions of O_2-NO connectivity (see Figure 3b). We therefore assign the m/z 30 and 32 peaks to the fraction of ions of O_2-NO connectivity from reaction (6), and the narrow m/z 46 peak, typical of weakly bound species and of an O-NO_2 connectivity, to the fraction of ions from reaction (7). Interestingly, at low source pressures the peaks of m/z 46 and m/z 30 become composite (Figure 4b), a feature traceable to fragmentation processes occurring through different potential-energy surfaces (PESs). Both peaks show a broad component whose intensity increases as the source pressure decreases. The peak of m/z 46 is particularly telling, since the same dish-topped metastable component observed in the case of the NO_3^+ model ion from reaction (5) can be deconvoluted and appears as a separate peak when floating the collision cell (see the inset). This feature is suggestive of the existence of two distinguishable species of O-NO_2 connectivity, one corresponding to the trigonal NO_3^+ model ion, and the other one corresponding to a weakly bound species that undergoes a near-threshold dissociation.

In summary, the mass spectrometric evidence points to the existence of two isomeric NO_4^+ ions of O_3-NO and O_2-NO_2 connectivity, and of three isomeric NO_3^+ ions, one of O_2-NO connectivity and two sharing the same O-NO_2 connectivity, but of different structures.

Neutralization of NO_3^+ and NO_3^- ions: We have extended the study to neutral species, utilizing three different ionic populations as charged precursors in separate neutralization reionization (NR) experiments: a) the "pure" population of trigonal NO_3^+ ions from reaction (5), b) the "pure" population of NO_3^+ ions of O_2-NO connectivity from reaction (6), and c) the mixed population from the NO_2/O_3 CI that contains, in addition to the above isomers, ions of O-NO_2 connectivity, as noted in the previous paragraph. Intense "recovery" peaks of m/z 62 are displayed by the $^+NR^+$ and $^+NR^-$ spectra of population a, consistent with the known stability of the trigonal $NO_3^{\bullet}$ radical. The same spectrum as that from $^+NR^-$ has been obtained from a charge reversal experiment, in which NO_3^- is formed in a single collisional event. Owing to the vertical character of the process, the result requires favorable Franck–Condon factors, namely similar equilibrium geometries of the NO_3^+ and the NO_3^- ions. We have demonstrated this independently by recording the $^-NR^+$ spectrum of the NO_3^- anion, obtained by negative-ion CI of methyl nitrate. The intense NO_3^+ ion from the reionization has been mass- and energy-selected and further analyzed by recording its CAD spectrum in the TOF section of the mass spectrometer. The CAD spectrum displays fragments of m/z 46 and m/z 30, confirming the structural assignment of the NO_3^+ population from reaction (5), and also showing that favorable Franck–Condon factors characterize the vertical transitions between the trigonal NO_3^+ ion, the $NO_3^{\bullet}$ trigonal radical, and the NO_3^- anion; this presupposes that the three species have similar structures.

With regard to population b, it is noteworthy that recovery peaks have also been obtained in the $^+NR^+$ spectra of different isotopomers of the $[O_2(NO)]^+$ ion (m/z 62), namely $[^{18}O_2(NO)]^+$ and $[^{18}O_2(^{15}NO)]^+$, of m/z 66 and 67, respectively. Although the spectrum is not intense and obtaining an acceptable S/N ratio requires averaging at least 400 scans (Figure 5), it proves to be completely different from that of the trigonal ion, the intensity of the recovery peak being comparable to those of the fragments of m/z 30, 32 and 31 (the last doubly charged). As to the $^+NR^-$ experiment, no detectable spectrum, and therefore no recovery peak, was obtained, owing to the insufficient intensity of the initial signal. The fragments observed in the $^+NR^+$ spectrum of the labeled precursors confirm the lack of isotopic mixing already observed in the CAD spectrum, and the absence of the distinctive peak of the trigonal NO_3^+ ion (m/z 46) rules out any isomerization of the neutral species occurring in the $\approx$1 μs interval between the neutralization and the reionization events.

Finally, depending on the experimental conditions previously illustrated, the NR spectra of population c are reminiscent of those typical of populations a and/or b, and display no features typical of the loosely-bound adduct of O-NO_2 connectivity, which most likely has no stable neutral counterpart.

  0947-6539/02/0824-5687 $ 20.00+.50/0

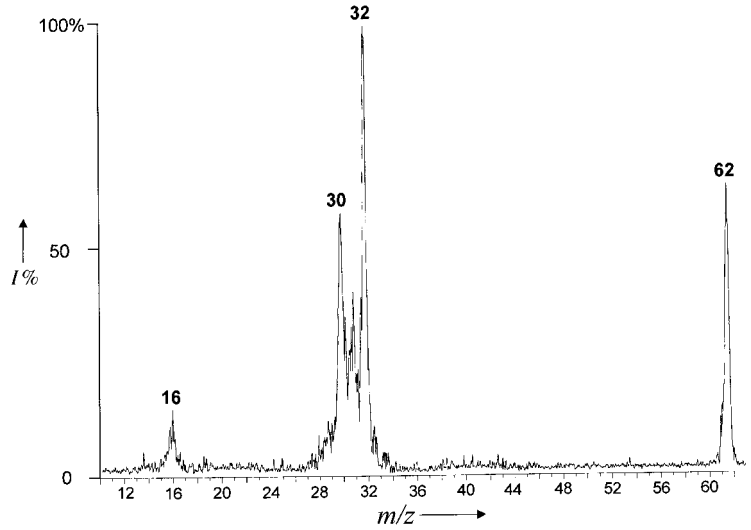

Figure 5. $^{+}NR^{+}$ mass spectrum of the NO_3^+ ion (m/z 62) from the NO/O_2 CI, see text. The peak of m/z 31 is assigned to the NO_3^{2+} ion.

Computational results: We have explored the B3LYP and CCSD(T) potential-energy surface (PES) of the NO_5^+ and NO_4^+ ions, and found the minima whose structure is reported in Figure 6. The ground state NO_5^+ ion **1** is a singlet that has

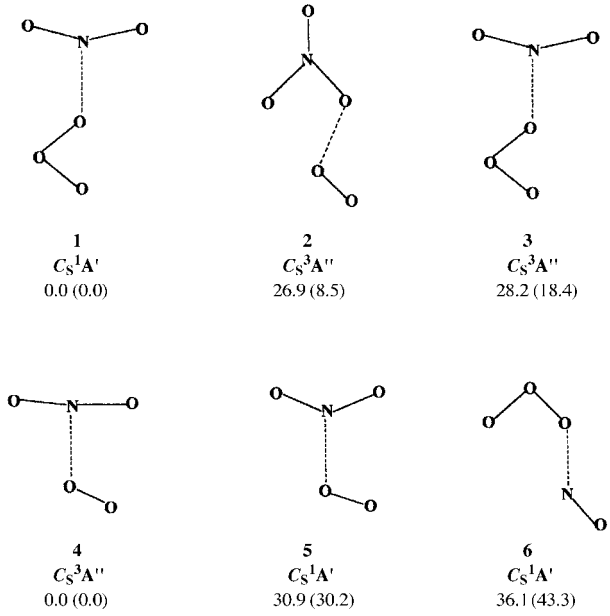

Figure 6. Optimized geometries of the minima localized on the potential energy surface of the NO_5^+ ion (**1**, **2**, and **3**) and of the NO_4^+ ion (**4**, **5**, and **6**). Relative energies at the CCSD(T) level (B3LYP in parentheses) are reported.

the structure of a NO_2^+-O_3 adduct, with a binding energy (BE) of 7.2 and 7.0 kcal mol^{-1} at the CCSD(T) and B3LYP levels of theory, respectively (Table 1). Two triplet species, with the structure of NO_3^+-O_2 (**2**) and NO_2^+-O_3 (**3**) adducts, respectively, have also been localized at higher energy. The most stable species on the PES of the NO_4^+ ion is the triplet **4**, which has the structure of an adduct between NO_2^+ and O_2, with a BE of 3.5 and 2.7 kcal mol^{-1} at 298 K at the CCSD(T) and B3LYP levels of theory, respectively (Table 1). At higher energy there is the singlet **5** with the same connectivity, but differing as to the O-N-O angle of the nitro group. Finally, at still higher energy, singlet **6** shows the O_3-NO connectivity, and its dissociation into NO^+ and O_3 at 298 K is computed to require 8.1 and 15.3 kcal mol^{-1} at the CCSD(T) and B3LYP levels of theory, respectively. The two singlets **5** and **6** are connected by a transition state located 38.1 and 39.8 kcal mol^{-1} above **5** at the CCSD(T) and B3LYP levels of theory, respectively.

Consistent with previous results,[6] among the species characterized by three N–O bonds, our calculations identify two trigonal NO_3^+ ($^1A_1$) ions, the one of C_{2v} symmetry (**7**) being the most stable isomer, slightly lower in energy than **8**, which has D_{3h} symmetry (Figure 7). The $^3B_2$ species **9** lies only 14.5 kcal mol^{-1} higher in energy than **8** at the CCSD(T) level, consistent with the experimental value (see Table 1).[11] Our computational analysis at both levels of theory supports previous results that identified the $[OONO]^+$ ion **10** as the most stable isomer,[12] located 83.1 kcal mol^{-1} (CCSD(T)) below the D_{3h} cation **8**. A difference of 75.1 kcal mol^{-1} can be derived (see Table 1) from available experimental data[11, 13] and from the measured NO^+/O_2 binding energy (BE) of 2.9 ± 0.2 kcal mol^{-1}.[14] Our computed NO^+/O_2 BE value amounts to 9.2 kcal mol^{-1} at the B3LYP level and 2.9 kcal mol^{-1} at the CCSD(T) level (Table 1); the latter is in better agreement with the experimental value and also with other theoretical studies.[12] Two singlet species of C_s symmetry, *cis*-**11** and *trans*-**12**, have also been identified (Figure 7) that lie 23.8 and

Table 1. ΔH° changes [kcal mol^{-1}, 298 K] of selected reactions involving the species of interest.[a]

	CCSD(T)[b]	B3LYP[b]	Experimental[c]	Reaction
NO_5^+(**1**) → $NO_2^+ + O_3$	7.2	7.0		(1)
NO_4^+(**4**) → $NO_2^+ + O_2$	3.5	2.7		(4)
NO_4^+(**6**) → $NO^+ + O_3$	8.1	15.3		(2)
NO_3^+(**8**) → NO_3^+(**9**)	14.5	− 6.7	14.5	
NO_3^+(**10**) → NO_3^+(**8**)	83.1	95.2	75.1	
NO_3^+(**10**) → $NO^+ + O_2$	2.9	9.2	2.9	(6)
NO_3^+(**8**) → $NO_2^+ + O(^1D)$			26.6	
NO_3^+(**9**) → $NO_2^+ + O(^3P)$	− 41.8	− 29.0	− 33.2	
NO_3^+(**13**) → $NO_2^+ + O(^3P)$	5.5	5.2		
$NO_2^+ + O_3$ → NO_3^+(**9**) $+ O_2$	56.3	44.1	58.8	(7)
$NO_2 + O_3^+$ → NO_3^+(**8**) $+ O_2$			− 21.4	(8)
$NO_2 + O_3^+$ → NO_3^+(**9**) $+ O_2$			− 6.9	(8)
$NO^+ + O_3$ → NO_3^+(**10**) $+ O(^3P)$	11.8	5.9	22.7	(10)
$NO_2^+ + O_3$ → NO_4^+(**4**) $+ O(^3P)$	11.0	12.4		(3)
$NO_2^+ + O_3$ → NO_3^+(**13**) $+ O_2$	9.0	9.9		(7)

[a] See Figures 6, 7, 9, and 10. [b] This work. [c] Refs. [11, 13, 14].

  0947-6539/02/0824-5688 $ 20.00+.50/0 *Chem. Eur. J.* **2002**, *8*, No. 24

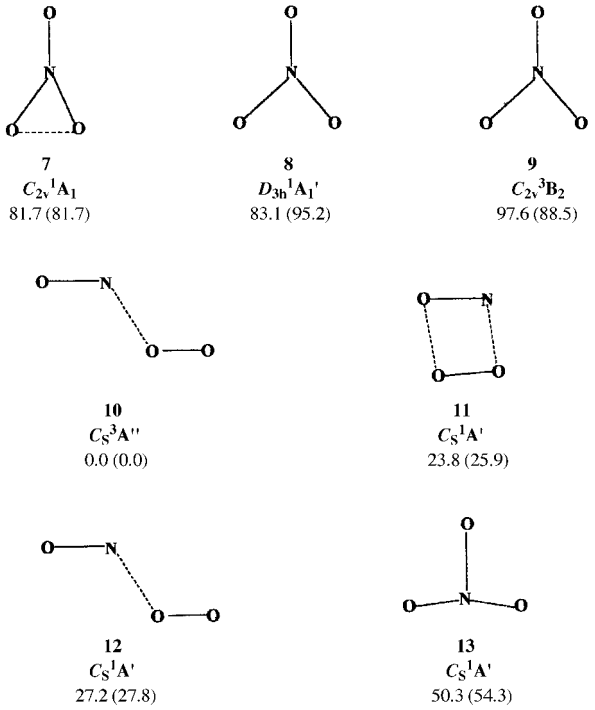

Figure 7. Optimized geometries of the minima localized on the potential energy surface of the NO_3^+ ion. Relative energies at the CCSD(T) level (B3LYP in parentheses) are reported.

27.2 kcal mol^{-1} above **10**, respectively, at the CCSD(T) level. Finally the triplet **13**, whose NO_2 group is nearly linear with a 176.7° angle, has been localized 32.8 kcal mol^{-1} lower in energy than ion **8** at the CCSD(T) level.

Figure 8 shows the optimized geometries and the relative stability of the species identified as minima on the PES of neutral NO_3. The symmetrical D_{3h} radical **14** is the most stable species at the B3LYP level, whereas the isomers **15** and **16** are computed to be slightly more stable at the CCSD(T) level, the discrepancy being traced to the symmetry-breaking problem,

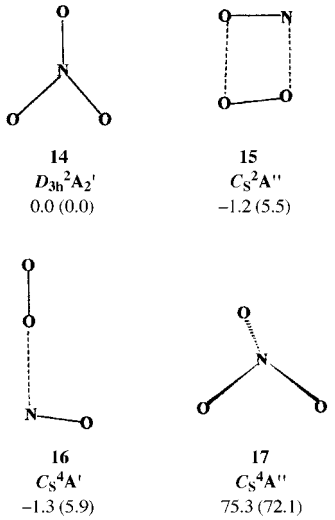

Figure 8. Optimized geometries of the minima localized on the potential energy surface of the $NO_3^{\bullet}$ radical. Relative energies at the CCSD(T) level (B3LYP in parentheses) are reported.

as recently suggested.[7f] The species **15** and **16**, characterized by an O-O-NO connectivity, are computed to be unbound both at the B3LYP and the CCSD(T) levels, once zero-point energy corrections are included, which would rule out their experimental detection. However, it should be pointed out that the above theoretical description of the $NO_3^{\bullet}$ system is affected by the computational problems associated with the multireferenced character of the wave function and the symmetry breaking effect, whose rigorous treatment definitely requires further theoretical work.

Discussion

Isomeric NO_x^+ species: The mass spectrometric and computational results reported in the previous section outline a coherent picture of the systems investigated.

As to the NO_5^+ ion, the CAD evidence, pointing to a O_3-NO_2 connectivity, would be consistent with the occurrence of both species **1** and **3**. However, formation of singlet **1** seems more likely, since that of the considerably less stable triplet **3** is expected to have to overcome a barrier arising from the change of multiplicity.

The NO_4^+ ion of O_3-NO connectivity from reaction (2) is likely to have the structure of species **6**, whereas the NO_4^+ ion of O_2-NO_2 connectivity from reaction (3) can have the structure of either ions **4** or **5**. Actually, on the basis of spin conservation arguments, reaction (3) is expected to yield only the triplet ion **4**, which can hardly be stabilized owing to its low NO_2^+/O_2 BE (Table 1). In addition, the experimental evidence indicates that in the NO_2/O_3 CI the competing reaction (2) of NO^+ is far more effective than the reaction (3) of NO_2^+. This becomes clearly evident when the abundances of the two competing reactant ions are comparable ($NO_2^+/NO^+ \approx 1{:}1$) and indeed no product from reaction (3) is detected. At lower pressures ($NO_2^+/NO^+ \approx 10{:}1$), despite the less efficient collisional stabilization, NO_4^+ ions of O_2-NO_2 connectivity are observed. This indicates that a product other than **4** is formed, and, hence, a process other than reaction (3) occurs. The most likely product is the singlet ion **5**, probably formed by a more energetically demanding process, an inference supported by the considerations discussed in the next paragraphs.

With regard to the NO_3^+ model ion, the MIKE and CAD evidence leads to the assignment of the same trigonal structure as that of the radical **14**. The most salient spectral feature is shown by the ionic fraction sampled by MIKE spectrometry, namely the dish-topped peak of m/z 46 relative to the metastable decomposition into NO_2^+ and O, characterized by a large KER. This is known to be related to the existence and the height of a barrier for the reverse reaction, namely NO_2^+ and $O \rightarrow NO_3^+$. Actually, the adiabatic dissociation of NO_3^+ is spin-forbidden from the NO_3^+ singlet state **8** to the ground state products, whereas the allowed dissociation into NO_2^+ and $O(^1D)$ is evaluated to be endothermic by 26.6 kcal mol^{-1} from available thermochemical data[13] (see Table 1). In this case, the barrier for the reverse reaction corresponds to the amount of energy exceeding the mere endothermicity, namely to the kinetic component of the

  0947-6539/02/0824-5689 $ 20.00+.50/0

barrier for the direct reaction. As to the NO_3^+ triplet **9**, also accessible under our experimental conditions given the energetics of the formation process, its decomposition to ground-state products is evaluated to be exothermic by 33.2 kcal mol^{-1} (see, for comparison, the computed values in Table 1). In this case, the barrier for the reverse reaction would correspond to the above exothermicity plus the kinetic barrier for the direct reaction. A larger KER is therefore expected from the decomposing triplet state (the same applies in the case of intersystem crossing) than from the singlet state. Although a truly accurate measurement of the KER is prevented by the low intensity of the metastable peak, it can be estimated to be $\approx$20 kcal mol^{-1}, a value that has to be taken as the lower limit of the barrier. Indeed, only a fraction of the energy released is converted into translational energy of the fragments, whereas a significant amount is expected to be deposited into the internal degrees of freedom of the NO_2^+ ion, formed with a large vibrational energy excess since the process involves relaxation to a linear structure of the initially bent NO_2 group. Hence, the dissociation of the triplet state, whose barrier for the reverse reaction amounts to at least 33 kcal mol^{-1}, appears consistent with the experimental value. In summary, whereas both **8** and **9** can be formed within the stable population sampled by CAD spectrometry, the evidence for their trigonal structure is provided by the salient spectral feature, namely the relatively large KER shown by the metastable NO_3^+ population assayed, which probably consists of triplet ions **9**. In any case, the kinetic barrier for the dissociation of NO_3^+ can reasonably be traced to the activation energy required to rearrange the *bent* NO_2 group into the ground-state *linear* NO_2^+ ion.

As mentioned before, ions of O-NO_2 connectivity, other than the trigonal model ion, are formed by reaction (7). Indeed, the trigonal ion cannot be formed by the reaction (7), which is highly endothermic and spin-allowed only for the triplet state (Table 1). However, at low pressures, in the absence of efficient collisional stabilization, reaction (8) can conceivably account for its formation (Table 1), thus explaining the broad components of the *m*/*z* 46 and 30 composite peaks, observed under these conditions and assigned to the model trigonal ion.

$$NO_2 + O_3^+ \rightarrow NO_3^+ + O_2 \qquad (8)$$

This implies that reaction (7) yields a different species, whose decomposition gives the narrow peak of *m*/*z* 46, typical of a weakly bound adduct. Accordingly, the best candidate is the triplet **13**, which is far more stable than the trigonal ion and liable to be formed without appreciable excess of internal energy. Moreover, it contains a *nearly linear* NO_2 group, which satisfactorily accounts for the negligible KER of its dissociation into NO_2^+ and O(^{3}P), endothermic by only 5.5 kcal mol^{-1} at the CCSD(T) level of theory (Table 1).

Finally, let us examine the NO_3^+ ions of O_2-NO connectivity from reaction (6). The NO^+/O_2 BE is too low to account for the stabilization of ion **10** from ground state NO^+ and O_2 species (Table 1). On the other hand, reactions other than (6) are unlikely to occur in the NO/O_2 plasma, as the weak ($<$5%) NO_2^+ ion present in the source undergoes no reaction with O_2. As to the **11** and **12** singlets, their BE with respect to the dissociation into NO^+ and the first O_2 singlet state ($a^1\Delta_g$) are expected to be close to that of the ground-state adducts, since the energy separation between O_2 ($a^1\Delta_g$) and the ground O_2 ($X^3\Sigma_g^-$), 22.6 kcal mol^{-1},[15] closely approaches the computed energy difference between **10** and **11**. An explanation for the detection of a more stable O_2-NO^+ adduct derives from the observation that in order to detect the NO_3^+ ion one has to work with a large ($\approx$4:1) excess of O_2 over NO. This suggests that O_2^+, rather than NO^+, might be the charged precursor. The higher clustering ability of O_2^+* in long-lived, electronically excited states, with respect to ground-state O_2^+, is well documented.[16] In the case of interest, we tentatively suggest the association of an O_2^+* and a NO molecule [reaction (9)].

$$O_2^{+*} + NO \rightarrow [O_2^{+*} \cdot NO] \rightarrow [O_2^{*} \cdot NO^+] \rightarrow [OO(NO)]^{+*} \qquad (9)$$

The excited adduct eventually formed would be characterized by a sufficiently high BE to allow its stabilization in the ion source. As a matter of fact, irrespective of their formation process, NO_3^+ ions of O_2-NO connectivity and sufficiently stable to exit the CI source, have been detected.[17]

In conclusion, the structural analysis of the NO_3^+ species suggests the occurrence of three isomers: 1) the trigonal cation, of O-NO_2 connectivity, with a *bent* NO_2 group, 2) the ion of O-NO_2 connectivity, with a *nearly linear* NO_2 group, and 3) the NO_3^+ peroxy-type cation, of O_2-NO connectivity.

Neutral NO_3 species: The trigonal $NO_3^{\cdot}$ radical is the only species so far positively identified and characterized. Of course, its stability in the isolated gas state is fully confirmed by the present NR results. Perhaps our finding, potentially most relevant to fundamental inorganic chemistry and to atmospheric chemistry, is the evidence for the existence of a different isomer, most likely of the peroxy-type connectivity as that assigned to its charged precursor. Previous computational studies characterized peroxy-type radicals as unstable, or marginally stable,[7a,c] and the latter prediction is confirmed by our own theoretical results that locate peroxy-type $NO_3^{\cdot}$ species in very shallow energy wells, prone to dissociation once zero-point energy corrections are included. The lack of theoretical support is compounded by the weakness of the NR spectrum and hence of the "recovery" peak detected. In this situation, in which isobaric contamination is ruled out by the correct isotopic shifts of the *m*/*z* ratio of the "recovery" peaks observed when differently labeled precursors are used, it cannot be rigorously excluded that the peroxy-type NO_3^+ population assayed may contain a very small fraction of ions of different connectivity, possibly arising from ionic isomerization processes. Although there is not the slightest indication for such a contamination, we conservatively take the NR results as a strong evidence for, rather than a proof-positive demonstration of, the existence of a peroxy-type radical, with a lifetime exceeding 1 μs. Hopefully, the present results will encourage further experimental, and especially theoretical, studies of this important class of radical(s).

0947-6539/02/0824-5690 $ 20.00+.50/0 *Chem. Eur. J.* **2002**, *8*, No. 24

General remarks on the reactivity of ionized NO_x/O_3 mixtures: Previous studies of the reactions occurring in ionized mixtures of ozone with a number of simple molecules have revealed the O- and O_2-donor ability of O_3 and/or its cation.[18] The reaction pattern is influenced by factors such as the ionization energy of the molecules involved and the stability of the primary charged adducts. The peculiar features of the NO^+/O_3 and NO_2^+/O_3 systems, deduced from the combination of our experimental and theoretical results, are illustrated in the energy profiles of Figures 9 and 10.

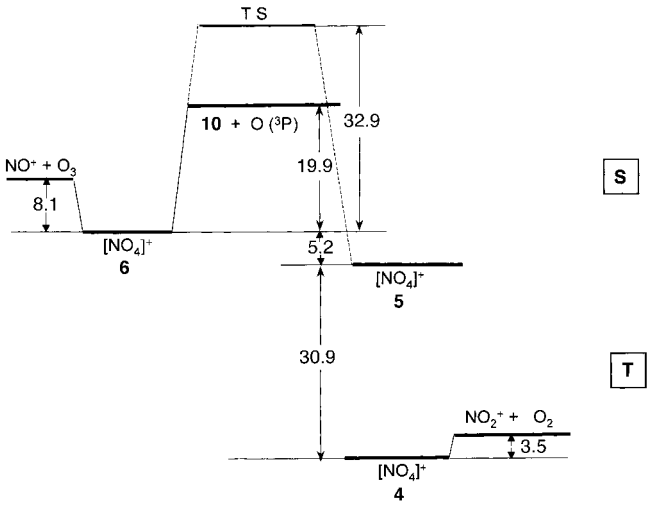

Figure 9. Energy profile (ΔH° [kcal mol^{-1}]) relevant to the NO^+/O_3 system, see text. The CCSD(T) values are reported, **T** denotes the triplet surface, **S** denotes the singlet surface.

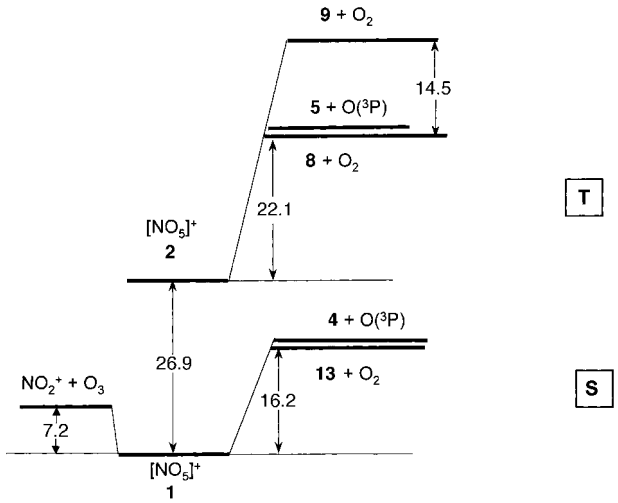

Figure 10. Energy profile (ΔH° [kcal mol^{-1}]) relevant to the NO_2^+/O_3 system, see text. The CCSD(T) values are reported, **T** denotes the triplet surface, **S** denotes the singlet surface.

Starting from NO^+, both the O_2- and O-transfer reactions (10) and (11) appear energetically unfavorable, despite the observation of the NO_4^+ intermediate [reaction (2)].

$$NO^+ + O_3 \rightarrow NO_3^+ + O \quad (10)$$

$$NO^+ + O_3 \rightarrow NO_2^+ + O_2 \quad (11)$$

Inspection of Figure 9 and Table 1 shows that O_2-transfer to NO^+, even to form the most stable NO_3^+ ion **10** of O_2-NO connectivity, is endothermic by 11.8 and 5.9 kcal mol^{-1} at the CCSD(T) and B3LYP levels, respectively. In contrast, a value of 22.7 kcal mol^{-1}, closer to the CCSD(T) one, can be derived from thermochemical and spectroscopic data.[11, 12] Moreover, the remarkably low dissociation energy of ion **10**, 2.9 kcal mol^{-1}, must be considered. Consistent with this picture, the NO_3^+ ion is very weak in the NO/O_3 CI plasma: the minor amount observed being traceable to the alternative reaction (6) with O_2, a minor process that, at low O_2 pressures, does not significantly compete with the reaction (2) of NO^+ with O_3.

The O-transfer reaction (11), albeit highly exothermic (Figure 9), is probably hindered by spin-conservation and structural constraints. In theory, one would expect that reaction (11) requires the intermediacy of a NO_4^+ ion of O_2-NO_2 connectivity, whereas the experimental evidence clearly indicates that in the NO/O_3 CI only one NO_4^+ isomer of O_3-NO connectivity, namely that characterized by structure **6**, is formed. Consistent with this view, the reaction between NO^+ and O_3 on the singlet surface gives the $[O_3\text{-}NO]^+$ adduct **6**, which has to overcome a barrier of 32.9 kcal mol^{-1} to form the species **5** of $[O_2\text{-}NO_2]^+$ connectivity. Thus, the two sections of the singlet surface, relevant to the formation of ions of O_3-NO and O_2-NO_2 connectivity, are only accessible starting from different reactants, and we will show below that ion **5** can actually be formed in the NO_2^+/O_3 system. Accordingly, in the NO/O_3/CI system, reaction (11) can be undergone, if at all, by only a minor fraction of the ions that have the required internal energy excess.

$$NO_2^+ + O_3 \rightarrow NO_4^+ (\mathbf{4}) + O \quad (3)$$

$$NO_2^+ + O_3 \rightarrow NO_3^+ (\mathbf{13}) + O_2 \quad (7)$$

Let us examine the reactions occurring in the NO_2^+/O_3 system. In this case, different O_2- and O-transfer reactions occur on the singlet and triplet surfaces, depending on the pressure regime adopted (Figure 10).

At high pressures ($NO_2^+/NO^+ \approx 1$), only the O-transfer reaction (7) is observed. Indeed, as previously noted, the endothermic O_2-transfer reaction (3) yielding the NO_4^+ ion **4** is not observed owing to the competing exothermic reaction (2) of NO^+ with O_3, yielding the NO_4^+ ion **6** (Figure 9). As to the O-transfer reaction (7), an inspection of Figure 10 and Table 1 shows that formation of the trigonal NO_3^+ ion is highly endothermic, whereas that of the NO_3^+ ion **13** via the singlet NO_5^+ ion **1**, is endothermic by 9 and 9.9 kcal mol^{-1} at the CCSD(T) and B3LYP levels, respectively (Table 1). Adopting the above values, even taking into account their presumably large uncertainty range, the reaction is likely to require vibrational excitation of the reactant ions. Indeed, consistent with the theoretical picture, the experimental evidence indicates that at high pressures, when the NO_5^+ intermediate is effectively stabilized and becomes detectable, NO_3^+ ions of O-NO_2 connectivity are formed having no energy excess and prone to prompt dissociation into NO_2^+ and $O(^3P)$. This supports the suggested assignment of structure **13**, which contains a nearly linear NO_2 group as ion **1**.

  0947-6539/02/0824-5691 $ 20.00+.50/0

At lower pressures, both the O_2- and O-transfer reactions, which yield NO_4^+ ions of O_2-NO_2 connectivity and the trigonal NO_3^+ ion, respectively, are experimentally detected. Reaction (8) between O_3^+ and NO_2 has already been considered as the possible route to the trigonal NO_3^+ ion. Accordingly, Figure 10 shows that access to the triplet surface from reactions more exothermic than reactions (3) and (7) could, in principle, yield the NO_5^+ ion **2** of O_2-NO_3 connectivity, with a preformed trigonal NO_3 group. Actually, whereas no NO_5^+ ion is detected under these conditions, probably as a result of inefficient collisional stabilization, its signature can be deduced from the products observed, namely the trigonal NO_3^+ ion and the NO_4^+ ion **5** of O_2-NO_2 connectivity [reaction (12)].

$$NO_2^+ + O_3 \rightarrow NO_4^+ (\mathbf{5}) + O \quad (12)$$

$$NO_2^+ + O_3 \rightarrow NO_3^+ (\mathbf{8},\mathbf{9}) + O_2 \quad (8)$$

Moreover, the expected charge exchange between O_3^+ and NO_2, exothermic by 65.7 kcal mol^{-1}, could generate NO_2^+ reactant ions in the triplet state, characterized by a bent geometry.[19] Thus the singlet and the triplet surfaces of Figure 10 are characterized by different geometries of the species involved: species with a *linear* nitro group, namely the NO_5^+ ion **1**, the NO_4^+ ion **4**, and the NO_3^+ ion **13** are located on the singlet surface; species with a *bent* nitro group, namely the NO_5^+ ion **2**, the NO_4^+ ion **5**, and the NO_3^+ ions **8** and **9**, are located on the triplet surface.

In conclusion, the complex reactivity pattern of ionized mixtures of ozone and NO_x oxides appears to be dominated by spin conservation and structural factors. In particular, the energy required to deform the linear NO_2 group into a bent geometry plays a crucial role in the reactions of interest.

Atmospheric implications: As to the relevance to atmospheric chemistry, ionization of NO_2/O_3 mixtures shows interesting outcomes. Under selective ionization conditions, reaction (7) on the singlet surface gives the *nearly linear* $[O\text{-}NO_2]^+$ ion **13**, that easily dissociates into NO_2^+ and $O(^3P)$ [reactions (13) and (14)].

$$NO_3^+ (\mathbf{13}) \rightarrow NO_2^+ + O(^3P) \quad (13)$$

$$O(^3P) + O_2 \xrightarrow{M} O_3 \quad (14)$$

Since potentially all ground-state O atoms can generate ozone by reaction with O_2, the overall process is a null cycle. In contrast, if the ionization process is unselective, the concomitant occurrence of reaction (8) on the triplet surface yields *bent* $[O\text{-}NO_2]^+$ ions. These are likely to undergo charge transfer to O_2 rather than dissociation with a resulting net loss of ozone. The reaction sequence occurring on the singlet surface is an ion-catalyzed dissociation of ozone that, unlike photolysis, gives ground-state products, so that NO_2 and ozone are neither produced nor destroyed. In contrast, the sequence occurring on the triplet surface could be relevant to the chemistry of the troposphere. Indeed, it has been shown that increasing concentrations of ozone and NO_2 are recorded by noon on smoggy days, and high local O_3 concentrations are reached in air ionized by lightning, and by natural or anthropogenic corona discharges. The process could prove effective in removing ozone and NO_2, and its product, the trigonal $NO_3^{\bullet}$ radical eventually formed, is atmospherically relevant as a night-time tropospheric oxidant, and a temporary odd-nitrogen reservoir.

Finally, a word of mention is deserved by the observation of the peroxy-type NO_3^+ ion. Although NO^+ and/or O_2^+ ions predominate in the E region of the ionosphere, ion–molecule reactions are generally more efficient at lower altitudes, namely in the D region, in which a complex positive-ion chemistry occurs. Whereas in the "quiet" D region NO^+ predominates, O_2^+ becomes dominant when the D region is "disturbed" by the impact of energetic particles from the sun, occurring both at night and during the day.[2] Excited states of O_2^+ could thus become available to the formation of the $[O_2(NO)]^{+*}$ adduct, whose BE is larger than that of the ground-state species. As a consequence, an additional route to the formation of cluster ions, characterized by different switching reactions between the neutrals involved, can be envisaged in this region.

Conclusion

Ionization of gaseous mixtures containing NO_x oxides and O_3 promotes a complex reaction pattern, whose theoretical and mass spectrometric study shows that the general tendency of ozone and its cation to undergo O_2- and O-transfer processes is limited in the systems of interest by spin-conservation and energetic constraints related to the change of geometry of the NO_2 moiety. Mass spectrometric evidence, supported by theoretical results, has led to the detection and characterization of the NO_5^+ ion, and of isomeric NO_4^+ and NO_3^+ species. In particular, in addition to the symmetrical trigonal cation, the mutually supporting experimental and theoretical results point to the formation in ionized NO_2/O_3 mixtures of a NO_3^+ isomer of O-NO_2 connectivity. This isomer contains a nearly linear NO_2 group, and is prone to dissociation into NO_2^+ and $O(^3P)$. A NO_3^+ ion, formally of peroxy-type structure, has been detected as a product from the ionization of NO/O_2 mixtures. As to the neutral chemistry, a most significant finding is the strong NR evidence for, if not the definitive demonstration of, the existence of a new $NO_3^{\bullet}$ isomer, in addition to the long known symmetrical, trigonal radical.

Experimental Section

Mass spectrometry: A ZABSpec oa-TOF mass spectrometer of EBE TOF configuration (Micromass, Manchester, UK) was used to generate the species of interest by chemical ionization performed at pressures ranging from ≈0.05 to 0.3 Torr. Typical operating conditions were as follows: accelerating voltage 8 kV, emission current 0.5 mA, repeller voltage 0 V, source temperature 150 °C. The mass-selected ions were structurally assayed by MIKE and CAD mass spectrometry. In the latter case, He was admitted into the collision cell to such a pressure as to reduce the beam intensity to 70 % of its original value. Multistage mass spectrometry (MS^3) experiments were performed by recording the CAD/TOF spectra of mass-selected daughter ions. The KER were measured by averaging ≈400 scans

0947-6539/02/0824-5692 $ 20.00+.50/0 *Chem. Eur. J.* **2002**, *8*, No. 24

at the energy resolution of 2.5 eV of the main beam width. The NRMS experiments were performed with projectile ions accelerated to 6–8 kV by collision with CH_4 in the first gas cell. After deflection of all the ions, the neutrals were reionized by collision with O_2 in the second gas cell. All gases and the other chemicals utilized were research-grade products from commercial sources with a stated purity in excess of 99.99% and were used without further purification. $^{18}O_2$ (^{18}O atoms 99%) was purchased from ICON, and ^{15}NO (^{15}N atoms 99%) was purchased from Aldrich. Ozone was prepared by passing UHP-grade oxygen (Matheson 99.95 mol%) through a commercial ozonizer, collected in a silica trap cooled to 77 K, and released upon controlled warming of the trap. The $NO_3^{\bullet}$ radical was generated in situ by mixing nitrogen dioxide with excess ozone in a flow system.

Computational details: Density functional theory, with the hybrid[21] B3LYP functional,[22] was used to localize the stationary points of the investigated systems and to evaluate the vibrational frequencies. Although it is well known that density functional methods that use nonhybrid functionals sometimes tend to overestimate bond lengths,[23] hybrid functionals, such as B3LYP, usually provide geometrical parameters in excellent agreement with experiment.[24] Single-point energy calculations at the optimized geometries were performed with the coupled-cluster single- and double-excitation method[25] with a perturbational estimate of the triple excitations [CCSD(T)] approach[26] in order to include extensive correlation contributions.[27] Transition states were located with the synchronous transit-guided quasi-Newton method from to Schlegel and co-workers.[28] The 6–311+G(3d) basis set[29] was used. Zero-point energy corrections evaluated at B3LYP/6–311+G(3d) level were added to the CCSD(T) energies. The 0 K total energies of the species of interest were corrected to 298 K by adding translational, rotational, and vibrational contributions. The absolute entropies were calculated with standard statistical-mechanical procedures from scaled harmonic frequencies and moments of inertia relative to B3LYP/6–311+G(3d) optimized geometries. All calculations were performed with Gaussian 98.[30]

Acknowledgements

Financial support was provided by the Rome University "La Sapienza", the Perugia University, the Ministero dell'Istruzione, Università e della Ricerca (MIUR), and Consiglio Nazionale delle Ricerche (CNR).

[1] a) F.Cacace, R. Cipollini, G. de Petris, F. Pepi, M. Rosi, A. Sgamellotti, *Inorg. Chem.* **1998**, *37*, 1398; b) F. Cacace, G. de Petris, F. Pepi, M. Rosi, A. Troiani, *Chem. Eur. J.* **2000**, *6*, 2572; c) F. Cacace, G. de Petris, M. Rosi, A. Troiani, *J. Phys. Chem.* **2001**, *105*, 1144; d) F. Cacace, G. de Petris , M. Rosi, A. Troiani, *Angew. Chem.* **2001**, *113*, 1992; *Angew. Chem. Int. Ed.* **2001**, *40*, 1938.

[2] R. P. Wayne, *Chemistry of Atmospheres*, 3rd ed., Clarendon Press, Oxford, **2000**.

[3] D. Smith, P. Spanel, *Mass Spectrom. Rev.* **1995**, *14*, 255.

[4] a) *Non-Thermal Plasma Techniques for Pollution Control* (Eds.: B. M. Penetrante, S. E. Schultheis), Springer, Berlin **1993**; b) M. Klein, D. W. Branston, G. Lins, M. Römheld, R. Seeböck, *Proc. Int. Conf. Gas Discharges Their Appl.* **1995**, *2*, 414; c) M. Baeva, H. Gier, A. Pott, J. Uhlenbusch, J. Höschele, J. Steinwandel, *Plasma Chem. Plasma Process.* **2001**, *21*, 225.

[5] I. Stefanovic, N. K. Bibinov, A. A. Deryugin, I. P. Vinogradov, A. P. Napartovich, K. Wiesemann, *Plasma Sources Sci. Technol.* **2001**, *10*, 406, and references therein.

[6] C. E. Miller, J. S. Francisco, *J. Phys. Chem.* **2001**, *105*, 1662.

[7] a) R. C. Boehm, L. L. Lohr, *J. Phys. Chem.* **1989**, *93*, 3430; b) R. D. Davy, H. F. Schaefer III, *J. Chem. Phys.* **1989**, *91*, 4410; c) V. R. Morris, S. C. Bhatia, J. H. Hall, Jr. *J. Phys. Chem.* **1990**, *94*, 7414; d) B. Kim, B. L. Hammond, W. A. Lester, Jr., H. S. Johnston, *Chem. Phys. Lett.* **1990**, *168*, 131; e) J. F. Stanton, J. Gauss, R. J. Bartlett, *J. Chem. Phys.* **1992**, *97*, 5554; f) W. Eisfeld, K. Morokuma, *J. Chem. Phys.* **2000**, *113*, 5587.

[8] a) W. A. Guillory, H. S. Johnston, *J. Am. Chem. Soc.* **1963**, *85*, 1695; b) W. A. Guillory, H. S. Johnston, *J. Chem. Phys.* **1965**, *42*, 2457; c) G. R. Smith, W. A. Guillory, *J. Mol. Spectrosc.* **1977**, *68*, 223.

[9] a) G. I. Gellene, R. F. Porter, *Acc. Chem. Res.* **1983**, *16*, 200; b) C. Wesdemiotis, F. W. McLafferty, *Chem. Rev.* **1987**, *87*, 485; c) J. K. Terlouw, H. Schwarz, *Angew. Chem.* **1987**, *99*, 805; *Angew. Chem. Int. Ed. Engl.* **1987**, *26*, 805; d) F. W. McLafferty, *Science* **1990**, *247*, 925; e) N. Goldberg, H. Schwarz, *Acc. Chem. Res.* **1994**, *27*, 347; f) C. A. Schalley, G. Hornung, D. Schröder, H. Schwarz, *Chem. Soc. Rev.* **1998**, *27*, 91.

[10] a) T. Ishiwata, I. Fujiwara, K. Naruge, K. Obi, I. Tanaka, *J. Phys. Chem.* **1983**, *87*, 1349; b) C. A. Cantrell, J. A. Davidson, R. E. Shetter, B. A. Anderson, J. G. Calvert, *J. Phys. Chem.* **1987**, *91*, 5858.

[11] D. Wang, P. Jiang, X. Qian, G. Hong, *J. Chem. Phys.* **1997**, *106*, 3003.

[12] E. P. F. Lee, T. G. Wright, *Chem. Phys. Lett.* **2000**, *318*, 196.

[13] a) P. S. Monks, L. J. Stief, M. Krauss, S. C. Kuo, Z. Zhang, R. B. Klemm, *J. Phys. Chem.* **1994**, *98*, 10017; b) H. F. Davis, B. Kim, H. S. Johnston, Y. T. Lee, *J. Phys. Chem.* **1993**, *97*, 2172; c) S. G. Lias, J. E. Bartmess, J. F. Liebman, J. L. Holmes, R. D. Levin, W. G. Mallard, *J. Phys. Chem. Ref. Data* **1988**, *17*, suppl 1.

[14] K. Hiraoka, S. Yamabe, *J. Chem. Phys.* **1991**, *95*, 6800.

[15] a) A. A. Frimer, *Singlet O_2*, CRC, Boca Raton, **1985**; b) A. P. Sohaap, *Singlet Molecular Oxygen*, Dowden, Hutchinson and Ross, Stroudsburg, **1976**; c) H. H. Wasserman, R. W. Murray, *Singlet Oxygen*, Academic Press, New York, **1979**.

[16] F. Cacace, G. de Petris, M. Rosi, A. Troiani, *Chem. Eur. J.* **2002**, *8*, 3653.

[17] Actually, our experimental evidence only points to the presence of a NO group in the structure, and does not allow a choice between the O_2-NO and the NO-O_2 connectivity. Species of N-O-O-O connectivity have been localized by our theoretical calculations on the singlet and triplet surfaces of NO_3^+. However, they lie at higher energy than those of ON-O-O, and are thus less stable with respect to dissociation.

[18] a) G. de Petris, *Acc. Chem. Res.* **2002**, *35*, 305; b) M. A. Mendes, L. A. B. Moraes, R. Sparrapan, M. N. Eberlin, R. Kostianen, T. Kotihao, *J. Am. Chem. Soc.* **1998**, *120*, 7869.

[19] K. Shibuya, S. Suzuki, T. Imamura, I. Koyano, *J. Phys. Chem.* **1997**, *101*, 685.

[20] A. D. Becke, *J. Phys. Chem.* **1993**, *98*, 5648.

[21] P. J. Stevens, F. J. Devlin, C. F. Chablowski, M. J. Frisch, *J. Phys. Chem.* **1994**, 98, 11623.

[22] B. Mannfors, J. T. Koskinen, L.-O. Pietila, L. Ahjopalo, *J. Molec. Struct. (THEOCHEM)* **1997**, *39*, 393.

[23] C. W. Bauschlicher, A. Ricca, H. Partridge, S. R. Langhoff, *Recent Advances in Density Functional Theory* (Ed.: D. P. Chong), World Scientific Publishing, Singapore **1997**, Part II.

[24] R. J. Bartlett, *Annu. Rev. Phys. Chem.* **1981**, *32*, 359.

[25] K. Raghavachari, G. W. Trucks, J. A. Pople, M. Head-Gordon, *Chem. Phys Lett.* **1989**, *157*, 479.

[26] J. Olsen, P. Jorgensen, H. Koch, A. Balkova, R. J. Bartlett, *J. Chem. Phys.* **1996**, *104*, 8007.

[27] a) C. Peng, H. B. Schlegel, *Israel J. Chem.* **1993**, *33*, 449; b) C. Peng, P. Y. Ayala, H. B. Schlegel, M. J. Frisch, *J. Comp. Chem.* **1996**, *17*, 49.

[28] a) R. Krishnam, J. S. Binkley, R. Seeger, J. A. Pople, *J. Chem. Phys.* **1980**, *72*, 650; b) A. D. McLean, G. S. Chandler, *J. Chem. Phys.* **1980**, *72*, 5639; c) T. Clark, J. Chandrasekhar, G. W. Spitznagel, P. von R. Schleyer, *J. Comput. Chem.* **1983**, *4*, 294; d) M. J. Frisch, J. A. Pople, J. S. Binkley, *J. Chem. Phys.* **1984**, *80*, 3265.

[29] M. J. Frisch, G. W. Trucks, H. B. Schlegel, G. E. Scuseria, M. A. Robb, J. R. Cheeseman, V. G. Zakrewski, J. A. Montgomery, Jr., R. E. Stratmann, J. C. Burant, S. Dapprich, J. M. Millam, A. D. Daniels, K. N. Kudin, M. C. Strain, O. Farkas, J. Tomasi, V. Barone, M. Cossi, R. Cammi, B. Mennucci, C. Pomelli, C. Adamo, S. Clifford, J. Ochterski, G. A. Petersson, P. Y. Ayala, Q. Cui, K. Morokuma, D. K. Malick, A. D. Rabuck, K. Raghavachari, K. X. Foresman, J. Cioslowski, J. V. Ortiz, A. G. Baboul, B. B. Stefanov, G. Liu, A. Liashenko, P. Piskorz, I. Komaromi, R. Gomperts, R. L. Martin, D. J. Fox, T. Keith, M. A. Al-Laham, C. Y. Peng, A. Nanayakkara, C. Gonzalez, M. Challacombe, P. M. W. Gill, B. Johnson, W. Chen, M. W. Wong, J. L. Andres, M. Head-Gordon, E. S. Repogle and J. A. Pople, Gaussian 98, Revision A.7, Gaussian, Inc., Pittsburgh PA, **1998**.

Received: May 22, 2002 [F4115]

  0947-6539/02/0824-5693 $ 20.00+.50/0